Geomechanics and Engineering, *Vol. 26, No. 4 (2021) 311-321*
https://doi.org/10.12989/gae.2021.26.4.311

Long-term behavior of earth pressure around a high-filled cut-and-cover tunnel

Sheng Li*[1], Yuchi Jianie[2a], I-Hsuan Ho[3b], Li Ma[1c], Guixia Ning[1d] and Changdan Wang[4e]

[1]*College of Civil Engineering, Lanzhou Jiaotong University, Lanzhou, Gansu, China*
[2]*Kunming Survey, Design and Research Institute Co., Ltd. of China Railway Eryuan Engineering Group, Kunming, Yunnan, China*
[3]*Harold Hamm School of Geology and Geological Engineering, University of North Dakota, 81 Cornell St. Stop. 8358, Grand Forks, ND 58202, U.S.A.*
[4]*Department of Urban Rail Transit and Railway Engineering, College of Transportation Engineering, Tongji University, Shanghai, China*

(Received April 25, 2020, Revised June 22, 2021, Accepted August 3, 2021)

Abstract. The Northwest Loess Plateau in China is mountainous and contains deep valleys which consist mostly of loess. Tunnels constructed in such deep valley and backfilled with soil are called high-filled cut-and-cover tunnels (HFCCT). Several studies have been conducted on HFCCT, but the creep behavior of loess backfill has not been fully explored. Post-construction settlement in loess is large, and it is difficult for stability to be reached in a short time. Therefore, it is necessary to predict long-term behavior of earth pressure around an HFCCT to ensure long-term safety. The primary purpose of this paper is to investigate changes in earth pressure and displacement of soil with time after the completion of the backfill process. This is achieved using FLAC^{3D} software (finite difference method). The results show that discrepancies in soil settlement and surface settlement will gradually increase and eventually reach stability. The distribution and value of earth pressure also becomes redistributed. Meanwhile, influencing factors such as slope angle and valley width gradually weaken with time, and only affect the time needed to reach stability.

Keywords: creep; earth pressure; *FLAC^{3D}*; high-filled cut-and-cover tunnel (HFCCT); post-construction settlement

1. Introduction

The long-term mechanical behavior of high-filled backfill soil is always a major concern in buried engineered structures. While there have been studies on earth pressure distribution for high-filled soils over pipes, culverts and cut-and-cover tunnels (CCT), the influence of creep behavior in backfill soil on earth pressure distribution is seldom investigated. The post-construction settlement caused by soil creep can change the relative settlement between the soil prism directly above the structure (internal soil column) and the adjacent soil prisms (external soil columns). This can generate frictional forces or shearing stresses that are either added to or subtracted from the dead weight of the central prism, and thus affect the resultant load on the structure. Therefore, it is necessary to predict the variation of earth pressure in high-filled structures.

∗Corresponding author, Professor
E-mail: lis@mail.lzjtu.cn
[a]Assistant Engineer
E-mail: 0618166@stu.lzjtu.edu.cn
[b]Associate Professor
E-mail: ihsuan.ho@und.edu
[c]Senior Lecturer
E-mail: mal@lzit.edu.cn
[d]Professor
E-mail: ningguixia@mail.lzjtu.cn
[e]Associate Professor
E-mail: 2008wangchangdan@tongji.edu.cn

The earliest studies of deeply buried culverts investigated the behavior of underground conduits through a series of analytical and experimental works (Marston and Anderson 1913, Marston 1930). Later studies show that the loads highly depended on the installation conditions that control the magnitude and direction of settling of the soil (Spangler 1950). In other words, embankment installations can have vertical earth pressure that exceeds the value of γh (Binger 1947, Trollope *et al.* 1963, Penman *et al.* 1975, Dasgupta and Sengupta 1991, Yang 2000, Bennett *et al.* 2005, Kim and Yoo 2005, Chen and Sun 2014) and trench installations can have earth pressure which is reduced by the amount of shearing stress exerted on the internal soil column (Vaslestad *et al.* 1993, Kim and Yoo 2005, McAffee and Valsangkar 2008, McGuigan and Valsangkar 2010, Chen and Sun 2014). More recently, several specifications (AASHTO 2010), which are based on Marston-Spangler (M-S) theory and empirical results, have been adopted in practical engineering for estimating earth pressure in culverts and pipe installations.

In terms of long-term sustainability, Spangler (1973) reported on load measurements on three pipe culverts conducted from 1927 to 1948 which the embankment material was sandy loam top soil containing gravel and some light clay. The results show that there is no substantial change in load over the 21-year period. Later, Vaslestad *et al.* (1993) described three full-scale tests. The first two tests, carried out on concrete pipes backfilled beneath high rock fills, indicates that both vertical stress and compression do not increase significantly after construction. In fact, there was a slight increase in deformation of the expanded polystyrene during the third full-scale test which used silty

ISSN: 2005-307X (Print), 2092-6219 (Online)

clay soil backfill. A later study by Sun *et al.* (2011) found that strain at the bottom of the culvert ceiling, recorded in situ over 5 years, gradually increases from <300 με to 351.29 με for the residual clay backfill. McAffee and Valsangkar (2008) compared the results of field data, centrifuge testing, and numerical modeling over a period of 2 years after embankment construction which consisted of a well-graded glacial till classified as clayey sand with gravel. The results show no marked changes in earth pressures or deformation. Overall, the long-term change of earth pressure in high-filled structures may be influenced by the creep properties of the backfill soil used (Arenaldi *et al.* 2019, Guo *et al.* 2020).

For HFCCT, a general formula was proposed for earth pressure above the HFCCT which considered several influencing factors (Li *et al.* 2014). Similar to deeply buried culverts and pipes (Meguid *et al.* 2017, Moghaddas *et al.* 2020, Santos *et al.* 2020), the load reduction measures that employ relatively low compacted soil and expanded polystyrene (EPS) have been found to be applicable for HFCCT (Li *et al.* 2020). The Northwest Loess Plateau in China usually applies loess, a convenient but sensitive material (Xie *et al.* 2018, Xue *et al.* 2019), in filling work (Hu *et al.* 2018, Zhu and Li 2020). As the backfilled loess is artificially reconstructed within a short time, the properties of the loess can be easily influenced by many conditions (Wang *et al.* 2019, Atashgahi *et al.* 2020, Prommin and Nuntasarn 2020), the post-construction settlement is usually large. Previous studies have shown the additional settlement caused by loess creep can be 1.4 m when a valley with 50 m deep is filled in by loess (Ge *et al.* 2015). The research how the backfill creep influences the earth pressures of HFCCT in the Northwest Loess Plateau is deficient. Therefore, this study used a finite difference method and focused on the creep behavior of high-filled soil, to investigate earth pressures and displacement around the CCT. Moreover, parametric studies were used to examine the creep response of different influencing factors, including the valley width and slope angle.

2. Numerical analysis

Numerical analysis was conducted using *FLAC*^{3D} software (Fast Lagrangian Analysis of Continua, Itasca Consulting Group, Inc., USA). This software uses finite difference methods to solve problems. In the program, the inbuilt creep mode was configured to simulate the creep behavior triggered by deviatoric stress, that the changes in earth pressure and displacement resulted from backfill soil creep were investigated.

2.1. Model establishment and parametric studies

To simplify the investigated volume, a typical finite-difference model was established with 1 m thick, as shown in Fig. 1. The model is 99 m tall and 90 m wide. It includes the depth of backfill (H = 61 m), the height of CCT (h = 11 m), the width of CCT (D = 12.8 m), the width of valley (B = 13.8 m), and the slope angle (β =70°). The backfill was divided into 7 layers: those to the sides of the CCT are

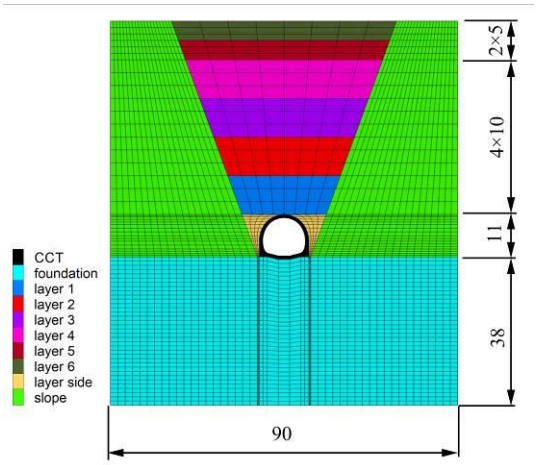

Fig. 1 Meshed *FLAC*^{3D} model for the HFCCT under investigation (units are meters)

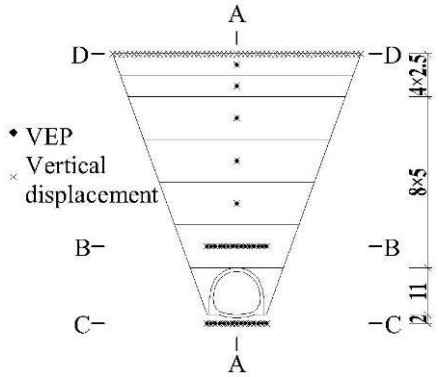

Fig. 2 Arrangement of Sections A-A, B-B, C-C, D-D and measuring points

referred to as layer side, those above the CCT are layer 1 to layer 6 (L1 – L6) from the top of CCT to the surface. In the model, the side boundaries were constrained only in the normal direction, while the bottom boundary was constrained in both normal and shear directions.

To obtain the changes in earth pressure around the CCT a certain number of measurement points were needed. Fig. 2 shows the positions of these points in various sections through the model. The measuring points in Sections B-B and C-C are used to record the changes in vertical earth pressure (VEP) and foundation earth pressure (FEP) with time around the CCT. Other measuring points were also arranged at the center of each layer (L1 to L6) in Section A-A to record differences in the VEP increment and post-construction settlement for each layer. Section D-D is used to record the change in post-construction settlement.

2.2 Properties of backfill

In this paper, the creep behavior of backfill is simulated by the Burgers model, based on the research done by Ge (2015). The research started with experimental tests on loess. In the tests, loess was obtained from a loess ridge in northwest of China. The specimen mainly consists of silt, mixed with a little silt clay. The physical properties of the samples are listed in Table 1.

Table 1 Physical properties of the loess samples (Ge *et al.* 2015)

Optimum moisture content (ω_0, %)	Maximum dry unit weight (ρ_d, g/cm^3)	Liquid limit (W_L, %)	Plastic limit (W_P, %)	Plasticity Index (I_P)	Specific gravity (G)
15.5	1.72	28	20.4	7.6	2.70

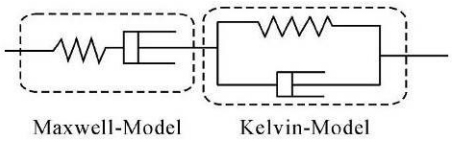

Fig. 3 Burgers creep behavior model used in this study, which consists of Maxwell model and a Kelvin model in series

Table 2 Parameters used in the Burgers model (Ge *et al.* 2015)

Stress (σ_0, kPa)	Maxwell elasticity (E_M, MPa)	Kelvin elasticity (E_K, MPa)	Maxwell viscosity (η_M, MPa·h)	Kelvin viscosity (η_K, MPa·h)	Coefficient of determination (R^2)
100	10.49	53.41	3672.22	17.65	0.9741
200	11.11	96.16	7628.26	39.65	0.9740
400	13.36	85.49	14775.71	33.10	0.9783
800	14.96	74.40	12002.48	8.91	0.9650
1200	15.54	99.35	23847.24	23.18	0.9676
1600	16.51	165.47	59164.77	136.43	0.9877
2000	17.84	292.44	145070.94	1047.98	0.9966

Table 3 Parameters for other materials (Li *et al.* 2020)

Material	Young's modulus (MPa)	Poisson's ratio	Cohesion (kPa)	Friction angle (°)	Unit weight (kN/m^3)
CCT	3×10^4	0.167	—	—	24
Foundation	50	0.25	78	32	22
Slope	4×10^3	0.2	—	—	20

A series of uniaxial compression creep tests were conducted. The experimental results were used to validate the Burgers model. The Burgers model consists of a Maxwell model and a Kelvin model in series, as shown in Fig. 3, and the constitutive equation of the model is expressed in Eq. (1). Taking a scheme for example (degree of compaction of 0.90, and the moisture content of 17.0%), the parameters of the loess material under various stress conditions used in the Burgers model are shown in Table 2. From the table, the coefficient of determination (R^2) of each load is shown, and all exceed 0.95, indicating that the Burgers model is applicable for loess. Details of the parameter acquisition process can be found in Ge (2015).

$$\varepsilon(t)=\frac{\sigma_0}{E_M}+\frac{\sigma_0}{\eta_M}t+\frac{\sigma_0}{E_K}\left[1-exp(-\frac{E_K}{\eta_K}t)\right] \quad (1)$$

where σ_0 is the initial stress; E_k is the elasticity of the Kelvin model; η_k is the viscosity of the Kelvin model; E_M is the elasticity of the Maxwell model; η_M is the viscosity of the Maxwell model; t is creep time and $\varepsilon(t)$ is the strain.

This paper applied the parameters in Table 2 to simulate the backfilled loess. In this study, iterative calculations were needed to obtain the real stress of each layer because different parameters were used for the backfill loess under different stress conditions in the model. The iterative processes were carried out by *FISH* language. It is an embedded programming language that enables the user to interact with and manipulate *FLAC^{3D}* models, defining new variables and functions as needed. Details are as follows:

Step 1: figure out the fitting functions between stress and other parameters according to Table 2;

Step 2: define the vertical stress of a meshed zone as the variable, and input the fitting functions, then the other parameters of the corresponding zone are worked out;

Step 3: reassign the zone with newly obtained parameters;

Step 4: use a loop command to repeat Step 2 and Step 3 for every zone that belongs to backfill;

Step 5: use a loop command to execute Step 4 once a timestep.

For other materials, the CCT and slope were modeled as linear elastic materials while the behavior of the foundation was simulated by the Mohr-Coulomb model (Li *et al.* 2020). Table 3 provides a summary of the parameters for the CCT, foundation and slope.

According to the calculations, the rate of the change of horizontal relative displacement at the bottom of the side wall is 0.01 mm/d (<0.2 mm/d) and the relative vertical displacement at the vault is 0.001 mm/d (<0.15 mm/d) (Code for Design of Railway Tunnel 2017). Therefore, it can be considered that the soil deformation is basically stable, and the total creep time was set at 8000 days.

3. Analysis of earth pressure

3.1 Earth pressure over time

VEP distribution of the backfill at different creeping times (0 d, 1000 d, 2000 d, 8000 d) are depicted in Fig. 4. When backfilling is completed (0 day), VEP is concentrated in the middle of the CCT (on the symmetric axis of CCT) because of the difference in rigidity between backfill and CCT. VEP decreases at the sides of the CCT because of the arching effect of soil between the CCT and slope. However, the earth pressure becomes redistributed as backfill creep is induced, and the stress concentration and soil arching effect both weaken with time. Results after 8000 days show that the earth pressure is equal at the same depth.

To obtain the VEP change of each layer with time, the VEP increment of each layer in Section A-A was extracted and compared (Fig. 5).

The increment of VEP with time is divided into three stages: linear increase, decelerating increase and stable. The VEP of each layer above the CCT basically becomes stable after 2000 days. Moreover, the maximum increment appears in L1 and the minimum increment in L6 because L1 is subjected to higher earth pressure, and creep behavior is evident. Note that the analytical results around the CCT based on VEP and FEP are described separately in the following sub-sections.

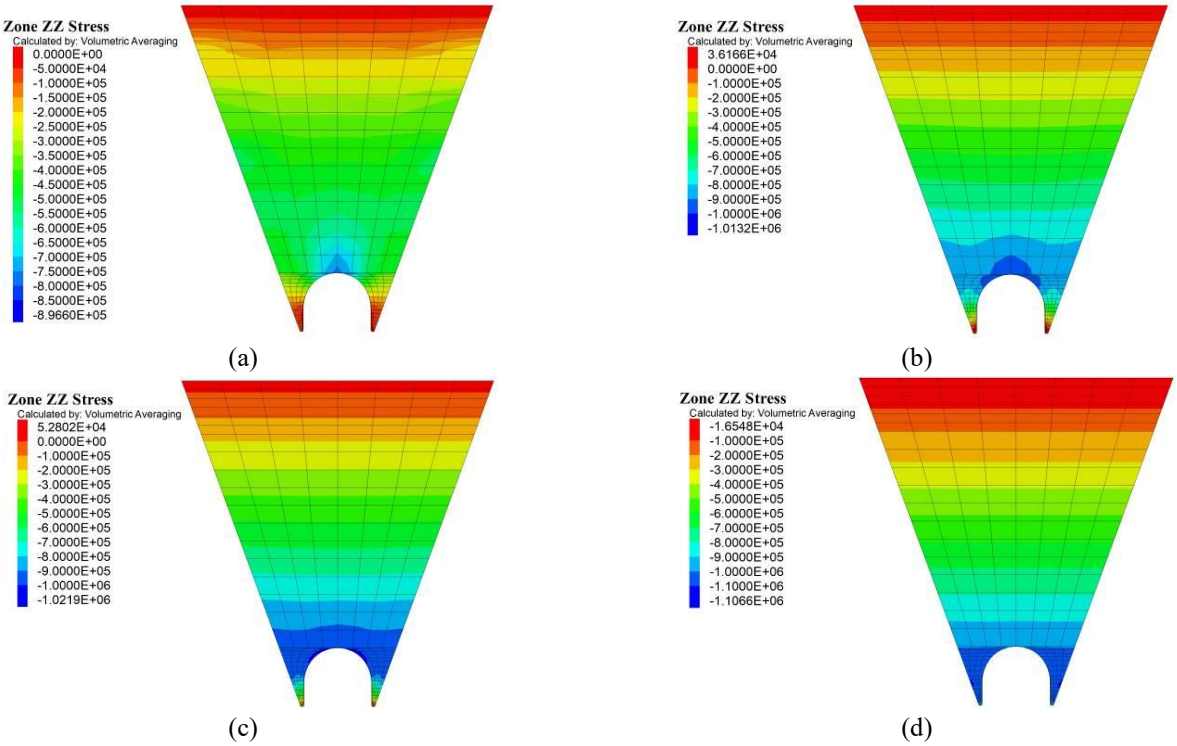

Fig. 4 VEP nephograms for (a) t = 0 d, (b) t = 1000 d, (c) t = 2000 d and (d) t = 8000 d

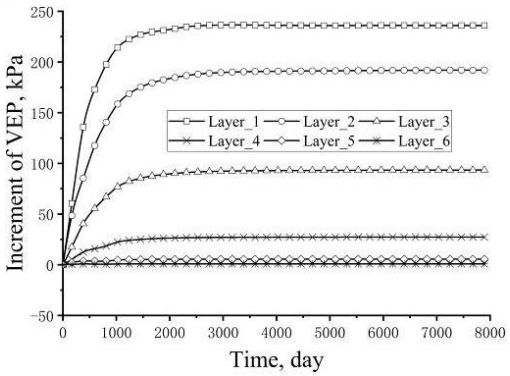

Fig. 5 Post-construction VEP increments of each layer over time in Section A-A

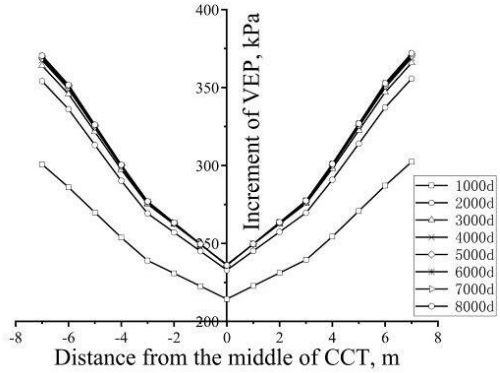

Fig. 7 VEP increment in Section B-B over 8000 days

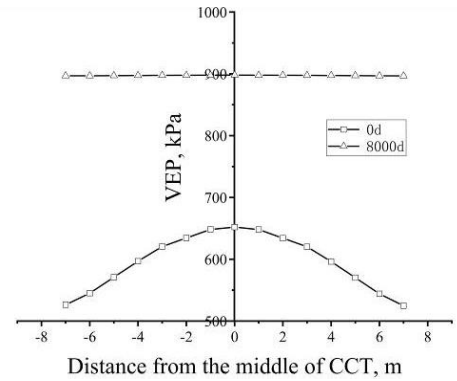

Fig. 6 VEP distribution in Section B-B at 0 day and 8000 days

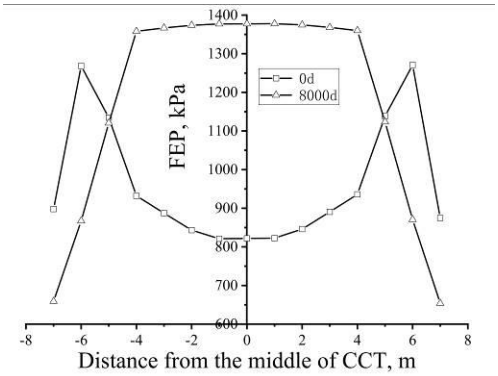

Fig. 8 FEP distribution in Section C-C at 0 day and 8000 days

3.2 VEP distribution above the cut-and-cover tunnel

A comparison of VEP distribution between 0 day and 8000 days in Section B-B is presented in Fig. 6. The increment of VEP from 0 day to 8000 days in Section B-B is presented in Fig. 7. At 0 day the VEP concentrates at the

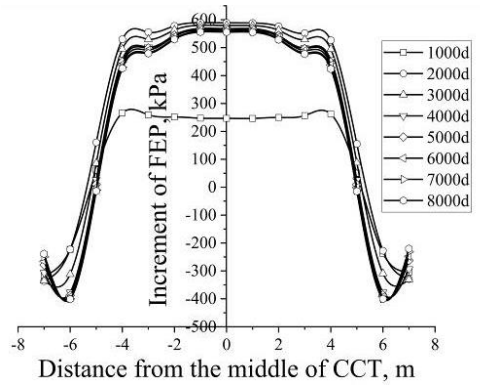

Fig. 9 FEP increment in Section C-C over 8000 days

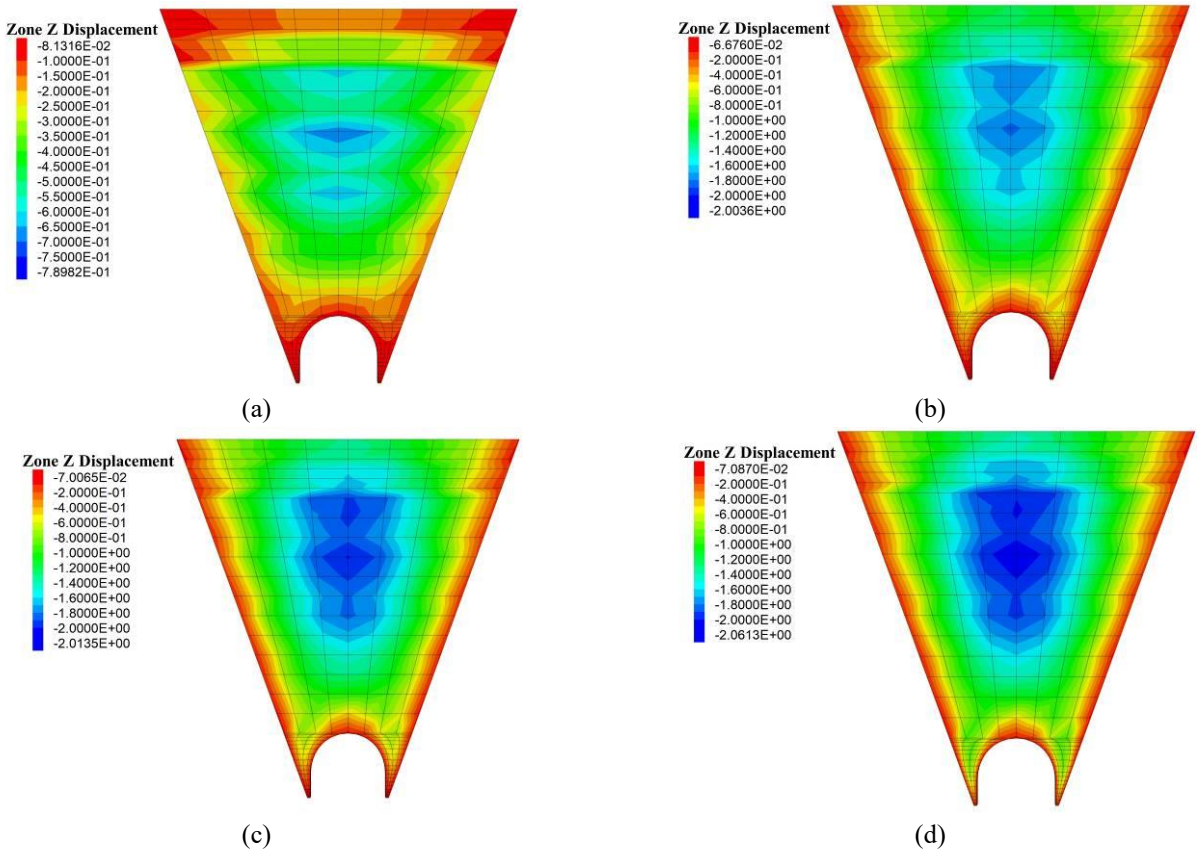

Fig. 10 Vertical displacement nephograms of backfill above the CCT for (a) t = 0 d, (b) t = 1000 d, (c) t = 2000 d and (d) t = 8000 d

center and decreases outward symmetrically because of differential settlement above the CCT. Note that the maximum difference in VEP is ~130 kPa (see Fig. 6). The minimum increment of VEP is located at the center and increases outward symmetrically at different times (see Fig. 7). After 8000 days, the VEP in Section B-B reaches 897 kPa (see Fig. 6), which is basically equivalent to the geostatic stress (900 kPa). Therefore, the earth pressure eventually equilibrates with the geostatic stress over time for the VEP in high backfill. Moreover, the increment of VEP reached 80% of the final state at 1000 days, and reached 95% at 2000 days. Hence, the first 2000 days can be considered the most significant time period in which creep occurs, and attention should be paid to settlement over this interval.

3.3. FEP at the base of the cut-and-cover tunnel

FEP distribution in Section C-C at 0 day and 8000 days is presented in Fig. 8, and the FEP increments from 0 day to 8000 days is presented in Fig. 9.

More displacement upward in bottom slab than that in the side walls results in the maximum FEP occurring at the side walls of CCT. Conversely, FEP at the center and both sides of CCT reaches only 2/3 of the peak (M distribution) after backfilling is completed (0 day). The FEP increases with time between the side walls of the CCT, and decreases outside of the side walls of the CCT. At 8000 days, FEP

between the two side walls is basically the same and decrease outwardly (inverse U distribution). Meanwhile, there is a delay in FEP reaching stability in Section C-C because the FEP is affected by the VEP that is not only in Section B-B, but in a wider range. The increment of FEP reached 50% of the final state at 1000 days, less than the VEP increment in Section B-B during the same phase.

4. Analysis of displacement

4.1 Displacement over time

The distribution of vertical displacement in the backfill at different creeping times (0 d, 1000 d, 2000 d, 8000 d), is represented in the nephograms in Fig. 10. When backfilling is completed (0 day) there is discontinuous vertical displacement at some interfaces of different layers. This may be related to the soil being filled in layers, and the timing of settlement of previous layers. However, this discontinuous displacement disappears with time; at 8000 days there is no such discontinuous settlement.

To investigate the changes in vertical displacement of each layer with time, the post-construction settlement of each layer in Section A-A was recorded (Fig. 11). The post-construction settlement of each layer with time is divided into three stages: linear increase, decelerated increase and stable. The post-construction settlement of each layer above the CCT basically stabilizes after 2000 days. Moreover, the maximum post-construction settlement is -1.4 m and

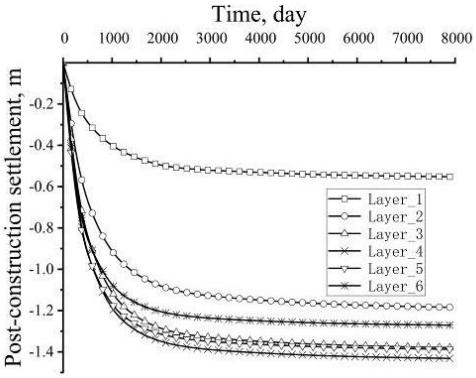

Fig. 11 Post-construction settlement of each layer in Section A-A over 8000 days

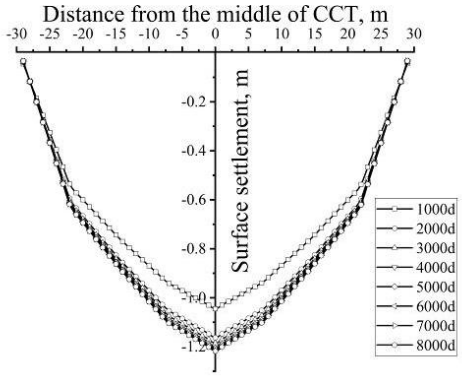

Fig. 12 Surface settlement in Section D-D over 8000 days

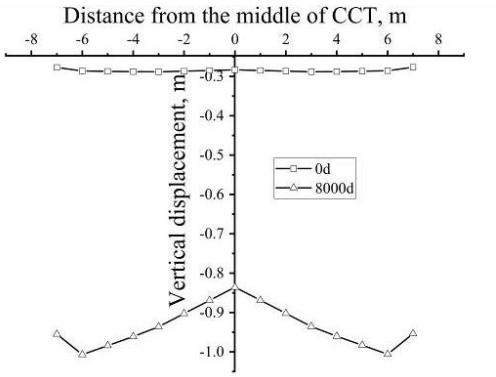

Fig. 13 Surface settlement in Section D-D over 8000 days

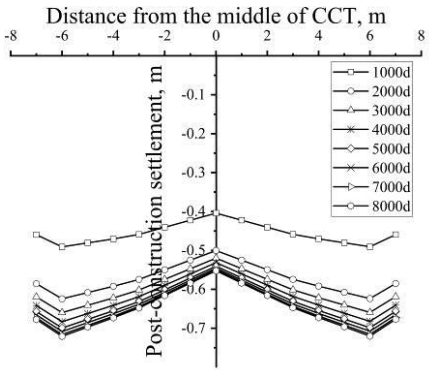

Fig. 14 Post-construction settlement in Section B-B over 8000 days

appears in layer 4, which is double the initial displacement (0 day). Therefore, the most significant period for post-construction settlement occurs before 2000 days.

4.2 Surface settlement

Fig. 12 illustrates surface settlement of backfill in Section D-D over 8000 days. The results show that the surface settlement is the greatest in the middle and then decreases linearly and symmetrically outward. The maximum settlement reaches 1.2 m, and 95% of the total settlement is essentially completed after 2000 days. Moreover, the surface settlement curve shows three different gradients because of the influences of the slope and the difference of rigidity between the backfill and CCT. Again, surface settlement can be considered most significant before 2000 days.

4.3 Displacement above the cut-and-cover tunnel

The distribution of vertical displacement in Section B-B at 0 day and 8000 days is shown in Fig. 13, and the post-construction settlement in Section B-B over 8000 days is shown in Fig. 14. In Section B-B, the post-construction settlement accounts for 66% of the total settlement. The post-construction deformation of backfill is relatively obvious even at the place around the rigid structure, CCT. Meanwhile, 91% of the total settlement is completed after 2000 days, the vertical displacement above the CCT can also be considered most significant before 2000 days.

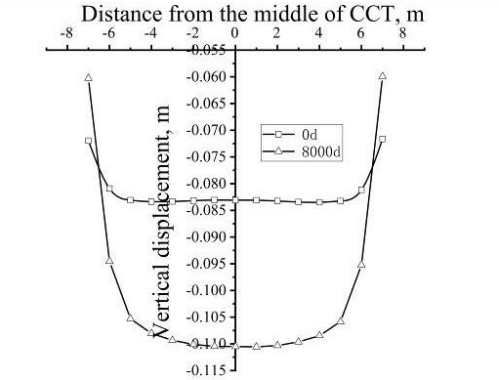

Fig. 14 Vertical displacement in Section C-C at 0 day and 8000 days

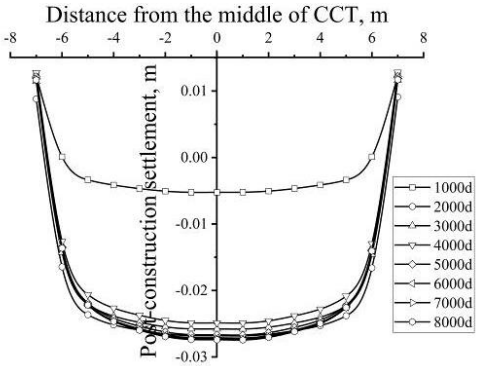

Fig. 15 Post-construction settlement in Section C-C over 8000 days

Moreover, at 0 day, the smallest vertical displacement occurs at the center above the CCT (-0.283 m). Outwards, the displacement symmetrically increases and peaks at the place about 0.5D from the central axis (-0.288 m), then decreases (W distribution). The discrepancy is 0.005 m, the settlement difference between the internal and external soil columns is limited at this moment. However, the discrepancy increases with time, and eventually reaches 0.17 m after 8000 days. The settlement difference between the internal and external soil columns gradually increases in post-construction.

4.4 Displacement at the base of the cut-and-cover tunnel

Fig. 15 shows the vertical displacement in Section C-C at 0 day and 8000 days. At 0 day, vertical displacement between the two side walls is about -0.83 m and the difference is <0.001 m, and decreases outward from the side walls (U distribution). The post-construction settlement between the two side walls increases, while the post-construction settlement outside the wall rebounds because of the squeezing action of the soil at the base of the CCT (Fig. 16). Post-construction settlement reaches -0.025 m, and 98% of the total settlement is completed after 2000 days. At 8000 days, the vertical displacement between the two side walls is about -0.11 m, while the displacement outside the wall rebounds to -0.06 m. This indicates that the post-construction settlement accounts for 25% of the total settlement, less than the proportion of post-construction settlement above the CCT because of the constraints of the slope and the CCT.

5. Parametric studies

The valley width and the slope angle may essentially impact the holding stress of the slope. In this paper, these two influential factors were varied as follows:

• valley widths: 1.0 times the CCT width (1.0D), 1.5D, 2.0D, and 3.0D, with the same slope angle (70°)

• slope angles: β = 40°, 50°, 70°, and 90°, with the same valley width (3.0D)

To assess the influence of the parameters qualitatively, the VEP and FEP at 1000 days were considered as evaluation indices.

5.1 Valley width

Nephograms of VEP in backfill with different valley widths (1.0D, 1.5D, 2.0D, 3.0D), are presented in Fig. 17. It can be seen that the stress concentration area above the CCT gradually increases and extends to both sides as the valley width increases. Meanwhile, the soil arching that is between the CCT and slope weakens and eventually disappears. Detailed calculation results based on VEP and FEP are discussed below.

5.1.1 VEP at the center above the cut-and-cover tunnel

The VEP of the central measuring point in Section B-B

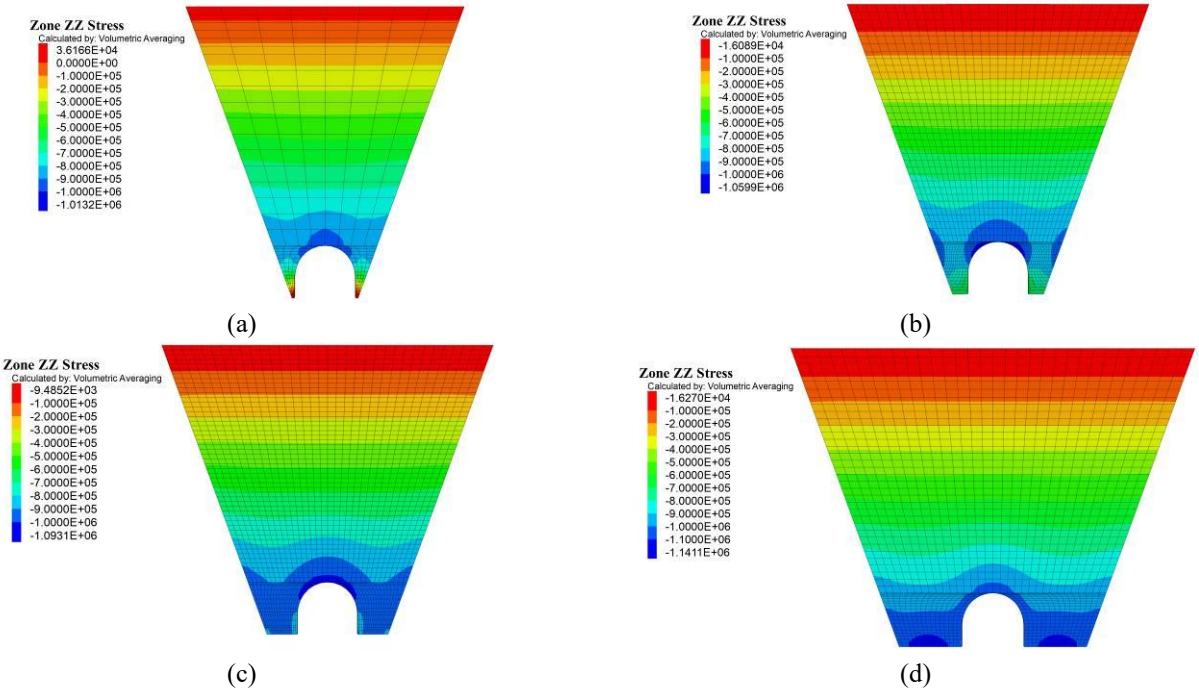

Fig. 16 VEP nephograms for different valley widths: (a) 1.0D, (b) 1.5D, (c) 2.0D and (d) 3.0D.

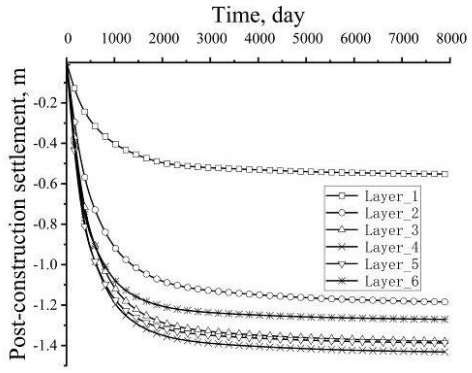

Fig. 17 Relationship between VEP and different valley widths at the central measuring point of Section B-B

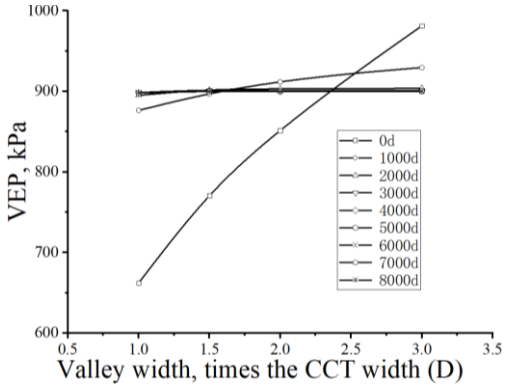

Fig. 18 Relationship between VEP and different valley widths at the central measuring point of Section B-B

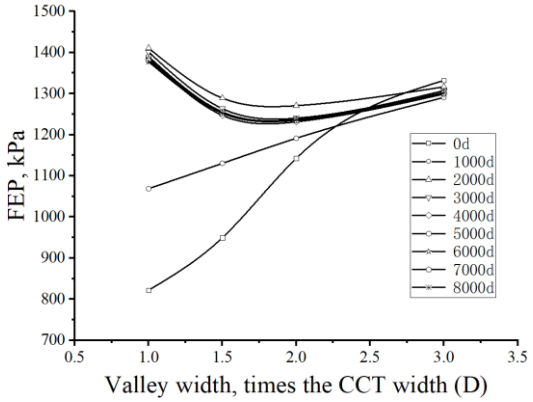

Fig. 19 Relationship between FEP and valley width at the central measuring point in Section C-C

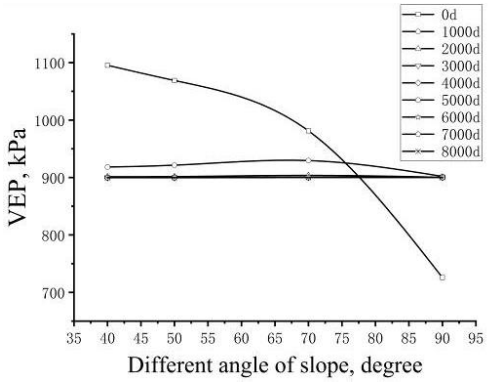

Fig. 20 Relationship between VEP and slope angle at the central measuring point in Section B-B

was extracted, and then plotted as a function of the different valley widths (Fig. 18). The results show that the VEP increases from 662 kPa to 981 kPa after backfilling is completed (0 day) when the valley width is varied from 1.0D to 3.0D. However, the influence of the valley width gradually decreases with time, having little effect after 2000 days. It could be concluded that VEP may be either greater

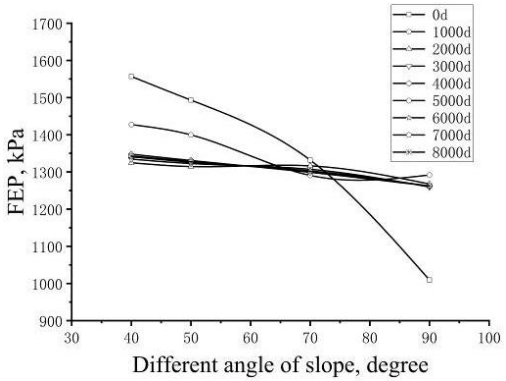

Fig. 21 Relationship between FEP and slope angle at the central measuring point in Section C-C

Fig. 22 The field test in an HFCCT engineering

or less than geostatic stress (900 kPa) at 0 day depending on the valley width, but VEP does in fact equilibrate with geostatic stress regardless of the valley width provided enough time elapses.

5.1.2 FEP at the center base of the cut-and-cover tunnel

The relationship between FEP at the central measuring point in Section C-C and the valley width is shown in Fig. 19. The FEP increases with increasing valley width from 0 day to 1000 days because of soil arching between the slope and CCT. Meanwhile, the FEP increases rapidly with time when the valley width varies between 1.0D and 2.0D. When valley width is 3.0D, the FEP remains essentially unchanged. Eventually, the FEP first decreases, and then increases with the increasing valley width, and the discrepancy is 11%.

5.2 Slope angle

5.2.1 VEP at the center above the cut-and-cover tunnel

The relationship between VEP and slope angle at the central measuring point in Section B-B is shown in Fig. 20. When slope angle is varied from 40° to 90°, there is a decline in VEP from 1095 kPa to 725 kPa when backfilling is completed. The VEP decreases for lower slope angles and increases for higher slope angles (0–1000 days), and eventually equilibrates with geostatic stress after 2000 days. The effect of slope angle on VEP is not significant after 2000 days.

5.2.2 FEP at the center base of the cut-and-cover tunnel

The influence of slope angle change on FEP at the central measuring point in Section C-C is shown in Fig. 21. The FEP decreases with increasing slope angle, as well as VEP. With time, the FEP fluctuates somewhat, but basically remains unchanged for slope angle $\beta = 70°$ and valley width B = 3.0D. Meanwhile, the FEP decreases for slope angles <70° and increases for slope angles >70°. Eventually, FEP declines as the slope angle increases, but the discrepancy is only 80 kPa, accounting for 6% of the total FEP.

6. Discussion

It is evident that the variation in earth pressure after completion of backfilling (0 day) is consistent with previous studies (Li *et al.* 2020). And, the earth pressure above the HFCCT varies over time based on the creep simulation. A field test (Li *et al.* 2014) has also observed this. The test was conducted on an HFCCT, as shown in Fig. 22. In the test, when the loess is filled back to 13.03 m high, the earth pressure above the CCT grows from 207.9 kPa to 225.8 kPa in 1 year. Therefore, attention should be paid to the changes of the highly backfilled loess in post-construction.

Generally, post-construction creep of high fill is a factor that must be considered when designing high fill projects, especially for clay. In this study, loess is applied in the HFCCT, differences in soil settlement between the internal and external soil columns, as well as surface settlement, are found to gradually increase, eventually reach stability. There is also clear redistribution of earth pressure over time. The influence of key factors on earth pressure (slope angle and valley width) gradually weaken with time, and these factors only affect the time required for earth pressure at different positions to reach stability.

It is acknowledged that this present study only examines the effects of creep in one backfill soil type (loess) on earth pressure around an HFCCT. Additionally, the creep of slopes and foundations is not considered because the trench is formed naturally. Also, several variables important in post-construction stability were not considered, such as degree of saturation and the ground water table. However, the results show that creep in backfill soil and resultant changes in earth pressure over time can be clearly identified for high-filled projects such as HFCCT.

7. Conclusions

Finite difference modeling using *FLAC*^{3D} was carried out to investigate the distribution of earth pressure and displacement around a CCT when considering soil creep. In addition, several influential factors, including the valley width and slope angle, were examined. The following conclusions can be drawn:

(1) The stress around the CCT is redistributed as a result of creep in the backfill soil. When the backfilling is

completed (0 day), the VEP concentrates at the center and decreases outward symmetrically (interval U-shaped distribution), the maximum FEP occurs at the side walls (M-shaped distribution). Earth pressure eventually reaches its final state, as the VEP equilibrates with geostatic stress (uniform distribution), and FEP has an interval U-shaped distribution. Meanwhile, the time required for earth pressure to reach stability is also different, and there is a delay in FEP reaching stability.

(2) The shape of vertical displacement distribution at various sections does not change with time. However, the settlement difference between the internal and external soil columns gradually increases with time. For example, the discrepancy changes from 0.005 m to 0.17 m in Section B-B and from 0.01 m to 0.05 m in Section C-C when the creep time varies from 0–8000 days. Moreover, the maximum surface settlement reaches 1.2 m after 2000 days.

(3) The influence of increasing the slope angle and lowering the valley width in terms of VEP reduction gradually disappears over time. However, the influence of slope angle and valley width on FEP decreases but always exists over time. Eventually, the FEP first decreases then increases with the valley width increase, and declines as the slope angle increases. The discrepancy is found to be ~6%–11%, which is not as great as when the backfill is completed (0 day).

Data availability statement

Data used in this work are available from the corresponding author by request.

Acknowledgments

This study was supported by the National Science Foundation of China (51668036, 51868041), General Projects of Scientific Research of High Education in Gansu (2017A-111), the Changjiang Scholars program and Innovative Research Team in the University (IRT_15R29), and the Energy Geomechanics Laboratory at the University of North Dakota, U.S.A.

References

AASHTO. (2010), AASHTO standard specifications for highway bridges, Washington, D.C., U.S.A.

Arenaldi Perisic, G., Ovalle, C. and Barrios, A. (2019), "Compressibility and creep of a diatomaceous soil.", *Eng. Geol*., **258**, 105145. https://doi.org/10.1016/j.enggeo.2019.105145.

Atashgahi, S., Tabarsa, A., Shahryari, A. and Hosseini, S.S. (2020), "Effect of carbonate precipitating bacteria on strength and hydraulic characteristics of loess soil", *B. Eng. Geol. Environ*., **79**, 4749-4763. https://doi.org/10.1007/s10064-020-01857-0.

Bennett, R.M., Wood, S.M., Drumm, E.C. and Rainwater, N.R. (2005), "Vertical loads on concrete box culverts under high embankments.", *J. Bridge Eng*., **10**(6), 643-649. http://doi.org/10.1061/(ASCE)1084-0702(2005)10:6(643).

Binger, W.V. (1947), "Discussion to 'Underground conduits-An appraisal of modern research'", *Proc. Am. Soc. Civ. Eng*., **73**, 1543-1545.

Chen, B.G. and Sun, L. (2014), "Performance of a reinforced concrete box culvert installed in trapezoidal trenches", *J. Bridge Eng*., **19**(1), 120-130. http://doi.org/10.1061/(ASCE)BE.1943-5592.0000494.

Code for design of railway tunnel (2017), China Railway Eryuan Engineering Group CO., Ltd.; Beijing, China (in Chinese).

Dasgupta, A. and Sengupta, B. (1991), "Large-scale model test on square box culvert backfilled with sand", *J. Geotech. Eng*., **117**(1), 156-161. https://doi.org/10.1061/(ASCE)0733-9410(1991)117:1(156).

Ge, M.M., Li, N., Zheng J.G., Zhu, C.H. and Ma, X.D. (2015), "Numerical analysis of the post-construction settlement regularity of loess-high filled embankment based on creep test", *J. Xi'an Univ. Technol*., **31**(3), 295-300+305 (in Chinese). https://doi.org/10.3969/j.issn.1006-4710.2015.03.008

Guo, W.B., Hu, B., Cheng, J.L. and Wang, B.F. (2020), "Modeling time-dependent behavior of hard sandstone using the DEM method.", *Geomech. Eng*., **20**(6), 517-525. https://doi.org/10.12989/gae.2020.20.6.517.

Hu, C.M., Wang, X.Y., Mei, Y., Yuan, Y.L. and Zhang, S.S. (2018), "Compaction techniques and construction parameters of loess as filling material", *Geomech. Eng*., **15**(6), 1143-1151. https://doi.org/10.12989/gae.2018.15.6.1143.

Kim, K. and Yoo, C.H. (2005), "Design loading on deeply buried box culverts.", *J. Geotech. Geoenviron. Eng*., **131**(1), 20-27. http://doi.org/10.1061/(ASCE)1090-0241(2005)131:1(20).

Li, S., Han, G.Q., Ho, I.H., Ma, L., Wang, Q.C. and Yu, B.T. (2020), "Coupled effect of cross-sectional shape and load reduction on high-filled cut-and-cover tunnels considering soil-structure interaction", *Int. J. Geomech*., **20**(7), 04020082. https://doi.org/10.1061/(ASCE)GM.1943-5622.0001696.

Li, S., Wang, Q.C., Ma, L., Li, J.X. and Li, W.L. (2014), "Model analysis of earth pressure load reduction and soil arch effect for high fill open cut tunnel in loess area", *China Civ. Eng. J*., **47**(7), 118-125 (in Chinese). https://doi.org/10.15951/j.tmgcxb.2014.07.040.

Marston, A. (1930), "The theory of external loads on closed conduits in the light of the latest experiments.", Bulletin No. 96; Iowa Engineering Experiment Station, Ames, Iowa, U.S.A.

Marston, A. and Anderson, A.O. (1913), "The theory of loads on pipes in ditch and tests of cement and clay drain tile and sever pipe.", Bulletin No. 31; Iowa Engineering Experiment Station, Ames, Iowa, U.S.A.

McAffee, R.P. and Valsangkar, A.J. (2008), "Field performance, centrifuge testing, and numerical modelling of an induced trench installation.", *Can. Geotech. J*., **45**(1), 85-101. https://doi.org/10.1139/T07-086.

McGuigan, B.L. and Valsangkar, A.J. (2010), "Centrifuge testing and numerical analysis of box culverts installed in induced trenches.", *Can. Geotech. J*., **47**(2), 147-163. https://doi.org/10.1139/T09-085.

Meguid, M.A., Hussein, M.G., Ahmed, M.R., Omeman, Z. and Whalen, J. (2017), "Investigation of soil-geosynthetic-structure interaction associated with induced trench installation", *Geotext. Geomembranes*, **45**(4), 320-330. https://doi.org/10.1016/j.geotexmem.2017.04.004.

Moghaddas Tafreshi, S.N., Joz Darabi, N. and Dawson, A.R. (2020), "Combining EPS geofoam with geocell to reduce buried pipe loads and trench surface rutting", *Geotext. Geomembranes*, **48**(3), 400-418. https://doi.org/10.1016/j.geotexmem.2019.12.011.

Penman, A.D.M., Charles, J.A., Nash, J.K.T.L. and Humphreys, J.D. (1975), "Performance of culvert under Winscar dam.", *Geotechnique*, **25**(4), 713-730.

https://doi.org/10.1680/geot.1975.25.4.713.
Prommin, T. and Nuntasarn, R. (2020), "Ultimate bearing capacity of collapsing Khon Kaen loess", *Int. J. GEOMATE*, **17**(63), 87-94. https://doi.org/10.21660/2019.63.14858.
Santos, R.R.V., Kang, J. and Park, J.S. (2020), "Effects of embedded trench installations using expanded polystyrene geofoam applied to buried corrugated steel arch structures", *Tunn. Undergr. Sp. Tech.*, **98**, 103323. https://doi.org/10.1016/j.tust.2020.103323.
Spangler, M.G. (1950), "A theory on loads on negative projecting conduits", *Proceedings of the 30th Annual Meeting of the Highway Research Board*, Washington, D.C., U.S.A., January.
Spangler, M.G. (1973), "Long-time measurement of loads on three pipe culverts.", *Proceedings of the 52nd Annual Meeting of the Highway Research Board*, Washington, D.C., U.S.A., January.
Sun, L., Hopkins, T. and Beckham, T. (2011), "Long-term monitoring of culvert load reduction using an imperfect ditch backfilled with geofoam", *Transp. Res. Rec.*, **2212**(1), 56-64. http://doi.org/10.3141/2212-06.
Trollope, D.H., Speedie, M.G. and Lee, I.K. (1963), "Pressure measurements on Tullaroop dam culvert", *Proceedings of the 4th Australia–New Zealand Conf. on Soil Mechanics and Foundation Engineering*, Perth, Australia, January.
Vaslestad, J., Johansen, T.H., Holm, W. (1993), "Load reduction on rigid culverts beneath high fills: Long-term behavior", Transportation Research Record 1415; Transportation Research Board, Washington, D.C., U.S.A.
Wang, X., Wang, J., Zhan, H., Li, P., Qiu, H. and Hu, S. (2019). "Moisture content effect on the creep behavior of loess for the catastrophic Baqiao landslide.", *CATENA*, **187**, 104371. https://doi.org/10.1016/j.catena.2019.104371.
Xie, X., Qi, S., Zhao, F. and Wang, D. (2018), "Creep behavior and the microstructural evolution of loess-like soil from Xi'an area, China", *Eng. Geol.*, **236**, 43-59. https://doi.org/10.1016/j.enggeo.2017.11.003.
Xue, Y., Zhang, X., Li, S.C., Qiu, D., Su, M., Xu, Z., Zhou, B. and Xia, T. (2019), "Sensitivity analysis of loess stability to physical and mechanical properties: Assessment model", *Int. J. Geomech.*, **19**(7), 06019012. https://doi.org/10.1061/(ASCE)GM.1943-5622.0001400.
Yang, M.Z. (2000), "Evaluation of factors affecting earth pressures on buried box culverts.", Ph.D. Dissertation, University of Tennessee, Knoxville, Tennessee, U.S.A.
Zhu, C. and Li, N. (2020), "Ranking of influence factors and control technologies for the post-construction settlement of loess high-filling embankments", *Comput. Geotech.*, **118**, 103320. https://doi.org/10.1016/j.compgeo.2019.103320.

CC